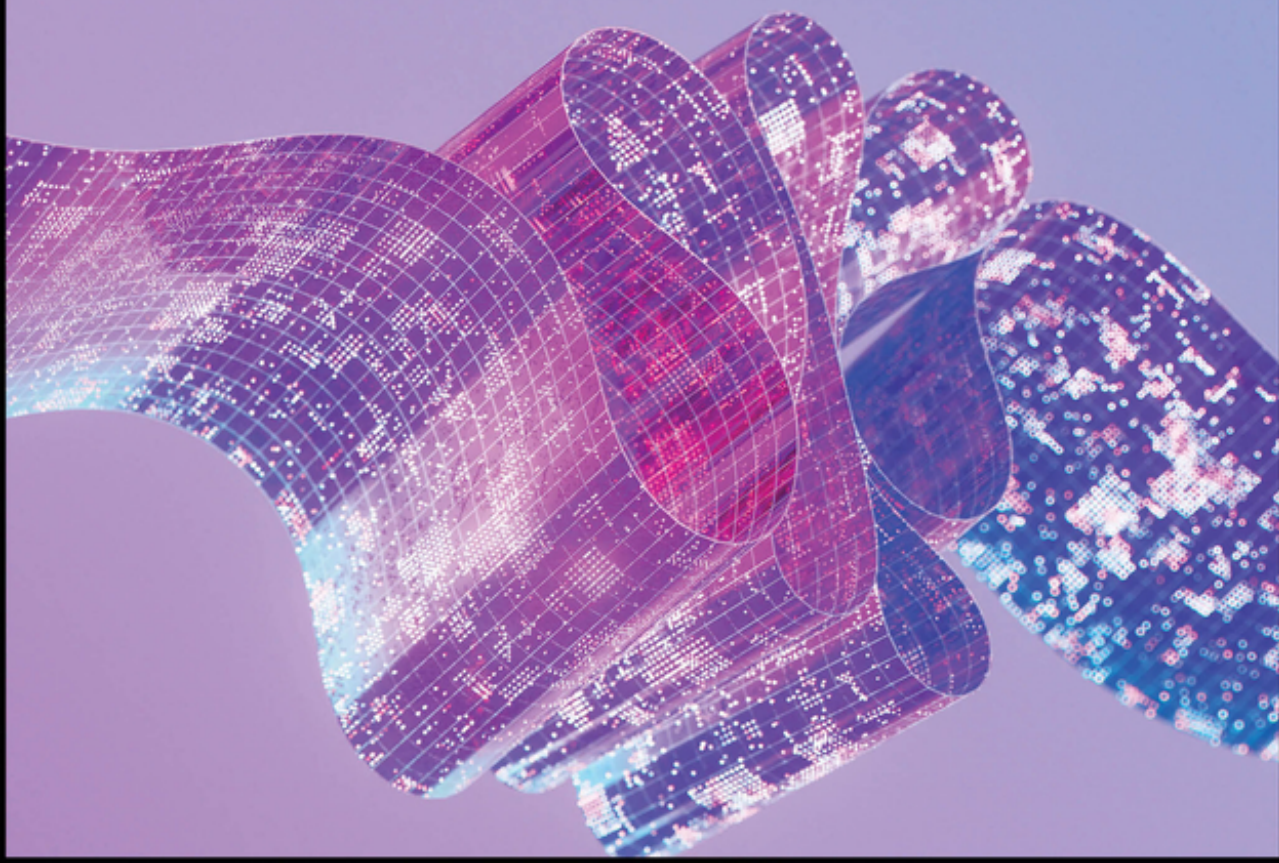


WILEY-VCH

Edited by Yong Zhu and Nanshu Lu

# Mechanics of Flexible and Stretchable Electronics





## **Mechanics of Flexible and Stretchable Electronics**



# **Mechanics of Flexible and Stretchable Electronics**

*Edited by Yong Zhu and Nanshu Lu*

## Editors

### *Prof. Yong Zhu*

North Carolina State University  
1840 Entrepreneur Dr.  
Raleigh  
NC 27695-7910  
USA

### *Prof. Nanshu Lu*

University of Texas  
2617 Wichita St., C0600  
Austin  
TX 78712-1221  
USA

**Cover Image:** © Eugene Mymrin/Getty Images

■ All books published by **WILEY-VCH** are carefully produced. Nevertheless, authors, editors, and publisher do not warrant the information contained in these books, including this book, to be free of errors. Readers are advised to keep in mind that statements, data, illustrations, procedural details or other items may inadvertently be inaccurate.

**Library of Congress Card No.:** applied for

### **British Library Cataloguing-in-Publication Data**

A catalogue record for this book is available from the British Library.

### **Bibliographic information published by the**

**Deutsche Nationalbibliothek** The Deutsche Nationalbibliothek lists this publication in the Deutsche Nationalbibliografie; detailed bibliographic data are available on the Internet at <<http://dnb.d-nb.de>>.

© 2025 WILEY-VCH GmbH, Boschstraße 12, 69469 Weinheim, Germany

All rights reserved, including rights for text and data mining and training of artificial technologies or similar technologies (including those of translation into other languages). No part of this book may be reproduced in any form – by photoprinting, microfilm, or any other means – nor transmitted or translated into a machine language without written permission from the publishers. Registered names, trademarks, etc. used in this book, even when not specifically marked as such, are not to be considered unprotected by law.

**Print ISBN:** 978-3-527-35219-7

**ePDF ISBN:** 978-3-527-84228-5

**ePub ISBN:** 978-3-527-84229-2

**oBook ISBN:** 978-3-527-84230-8

**Typesetting** Straive, Chennai, India

## Contents

**Preface** *xiii*

**Part I Materials** *1*

- 1 Extreme Mechanics of Hydrogels Toward *In Situ* Hydrogel Bioelectronics** *3*  
*Tsz H. Wong, Xuanhe Zhao, and Shaoting Lin*
- 1.1 Introduction *3*
- 1.2 Extreme Properties of Hydrogels by Polymer Network Design *5*
- 1.2.1 Elastic Modulus *6*
- 1.2.2 Fracture Toughness *8*
- 1.2.3 Fatigue Threshold *11*
- 1.2.4 Mass Transport *12*
- 1.3 Stretchable Hydrogel Conductors *14*
- 1.3.1 Multiscale Orthogonal Design *14*
- 1.3.2 Implementations of the Orthogonal Design *15*
- 1.4 Electrochemical Hydrogel Biosensors *18*
- 1.4.1 Selective Transport Design of Hydrogels *19*
- 1.4.2 Electrochemical Design of Hydrogel-2D Material Interfaces *20*
- 1.5 Flexible Hydrogel Biobattery *20*
- 1.5.1 Mechanical Energy Harvester *21*
- 1.5.2 Chemical Energy Harvesters *22*
- 1.5.3 Thermal Energy Harvesters *23*
- 1.6 Concluding Remarks *23*
- Acknowledgments *24*
- References *25*
- 2 Multiscale Mechanics of Metal Nanowire-Based Stretchable Electronics** *37*  
*Shuang Wu and Yong Zhu*
- 2.1 Introduction *37*
- 2.2 Metal NW-Based Flexible and Stretchable Electronics *38*

2.3	Mechanics of Individual NWs	39
2.3.1	Overview of Mechanics of Metal NWs	40
2.3.2	Mechanics of Single-Crystalline Metal NWs	40
2.3.3	Mechanics of Bi-Twinned Metal NWs	42
2.3.4	Mechanics of Penta-Twinned Metal NWs	43
2.4	Interfacial Mechanics of the NW–Polymer Interface	45
2.4.1	Classic Theory of Shear-Lag Analysis	45
2.4.2	Shear-Lag Analysis Considering Bonding Mechanisms	46
2.4.3	Fracture of NWs Due to Shear Stress Transfer	49
2.4.4	Elastoplastic Analysis of Metal NWs	51
2.5	Mechanical Design of Stretchable Structures	54
2.5.1	Buckle-Delamination Enabled Stretchable Silver Nanowire Conductors	54
2.5.2	A Highly Sensitive, Stretchable, and Robust Strain Sensor Based on Crack Advancing and Opening	55
2.6	Concluding Remarks	58
	Acknowledgments	59
	References	60
<b>3</b>	<b>Liquid Metal-Based Electronics</b>	<b>69</b>
	<i>Carmel Majidi</i>	
3.1	Introduction	69
3.1.1	Ga-Based Liquid Metals	69
3.1.2	Relevant Literature	71
3.2	LM Architectures	71
3.2.1	Microfluidic LM Channels	71
3.2.1.1	Printing-Based Deposition Methods	72
3.2.1.2	Direct LM Casting	73
3.2.2	LM-Coated Thin-Film Metal Traces	73
3.2.3	LM–Polymer Composites	74
3.2.4	Printable LM-Based Inks	76
3.3	Mechanics and Modeling	76
3.3.1	Microfluidic LM Strain Gauge	76
3.3.2	Microfluidic LM Pressure Sensor	77
3.3.3	LM–Polymer Composites	79
3.3.3.1	Electrical Permittivity and Thermal Conductivity	79
3.3.3.2	Electromechanical Coupling	79
3.3.3.3	Effective Young’s Modulus	80
3.4	Open Challenges and Future Directions	81
	References	82
<b>4</b>	<b>Mechanics of Two-Dimensional Materials</b>	<b>87</b>
	<i>Olugbenga Ogunbiyi and Yingchao Yang</i>	
4.1	Introduction	87
4.2	Nanoindentation Method	90



4.3	AFM-Enabled Nanoindentation	93
4.3.1	Setup of AFM-Enabled Nanoindentation	93
4.3.2	Mechanical Testing of 2D Materials	95
4.3.2.1	Mechanical Testing of Graphene	95
4.3.2.2	Mechanical Testing of Graphene Oxide (GO)	101
4.3.2.3	Mechanical Testing of MoS <sub>2</sub>	103
4.3.2.4	Mechanical Testing of WSe <sub>2</sub>	103
4.3.2.5	Mechanical Testing of <i>h</i> -BN	105
4.3.2.6	Mechanical Testing of Black Phosphor (BP)	107
4.4	<i>In Situ</i> Indentation in SEM	108
4.4.1	Raman Spectroscopy	110
4.5	Micro-/Nano-mechanical Devices	111
4.5.1	Category of Micromechanical Devices	111
4.5.1.1	Thermal Actuated Micromechanical Devices	111
4.5.1.2	Micromechanical Devices with Push–Pull Mechanism	112
4.5.2	Development of the “Dry-Transfer” Technique	113
4.5.3	Mechanical Testing of 2D Materials	115
4.5.3.1	Mechanical Testing of Graphene	115
4.5.3.2	Mechanical Testing of Rebar Graphene	117
4.5.3.3	Mechanical Testing of MoSe <sub>2</sub>	117
4.5.3.4	Mechanical Testing of <i>h</i> -BN	118
4.6	Piezoelectric Tube-Driven Testing in TEM	120
4.7	Bulge Testing	121
4.7.1	Depressurize Inside and Form a Concave Deflection in Film	121
4.7.2	Depressurize Outside and Form a Convex Deflection in Film	122
4.8	Electrostatic Force Triggered Drum Structure	124
4.9	Phonon Dispersion Measurement	125
4.10	Summary	126
4.10.1	Mechanical Testing Techniques	126
4.10.2	Mechanical Properties of 2D Materials	127
	Disclosure Statement	128
	References	128
<b>5</b>	<b>Mechanics of Flexible and Stretchable Organic Electronics</b>	<b>139</b>
	<i>Abdullah Al Shafe and Brendan T. O'Connor</i>	
5.1	Introduction	139
5.2	Mechanical Characterization Methods	140
5.2.1	Tensile Tests	141
5.2.2	Fracture Toughness	143
5.2.3	Thermomechanical Behavior	143
5.3	Material Design	145
5.3.1	Molecular Weight	145
5.3.2	Backbone and Side-Chain Design	146
5.3.3	Regioregularity and Crystallinity	147

5.3.4	Block Copolymers with Flexible and Stretchable Linkers	148
5.3.5	Crosslinking and Hydrogen Bonding	148
5.3.6	Additives and Blends	150
5.3.7	Organic Photovoltaic Considerations	152
5.4	Device Design	153
5.4.1	Neutral Axis and Ultrathin Devices	153
5.4.2	Film Thickness	153
5.4.3	Electrodes and Interlayers	155
5.4.4	Interfaces	155
5.4.5	Stretchable Device Architecture	156
5.5	Applications	156
5.6	Conclusion	159
	Acknowledgments	159
	References	160

## **Part II Design and Manufacturing** 171

<b>6</b>	<b>Structural Design of Flexible and Stretchable Electronics</b>	<b>173</b>
	<i>Zhaoqian Xie, Zichen Zhao, and Raudel Avila</i>	
6.1	Introduction	173
6.2	Design of Planar Stretchable and Flexible Structures	174
6.2.1	Wave/Wrinkle Structure Design	174
6.2.2	Island–Bridge Structure Design	177
6.2.2.1	Straight Interconnecting Island–Bridge Structure	178
6.2.2.2	Serpentine Interconnecting Island–Bridge Structure	180
6.2.2.3	Fractal-Inspired Interconnecting Island–Bridge Structure	186
6.3	Design of Three-Dimensional Flexible Electronic Structures	189
6.3.1	Helical Design	189
6.3.2	Origami-Inspired Design	190
6.3.3	Kirigami-Inspired Design	192
6.4	Design of Protective Structures for Flexible Electronic Devices	193
6.4.1	Strain Limited Structure Design	193
6.4.2	Strain Isolation Structure Design	195
	References	202
<b>7</b>	<b>Laser-Based Fabrication Process Development for Flexible and Stretchable Electronics</b>	<b>207</b>
	<i>Jung Jae Park, Minwoo Kim, and Seung Hwan Ko</i>	
7.1	Introduction	207
7.2	Representative Laser-Based Fabrication Process	208
7.3	Applications Based on Laser Fabrication	211
7.4	Perspectives and Conclusion	225
	Author Contributions	226
	References	226

<b>8</b>	<b>Electrospinning Manufacturing of Stretchable Electronics</b>	<b>235</b>
	<i>Yinhui Li, Kan Li, Yunlei Zhou, and YongAn Huang</i>	
8.1	Background	235
8.2	High-Precision Manufacturing	236
8.2.1	Inkjet Printing	236
8.2.2	EHD Printing	239
8.3	Electrospinning Stretchable Structure	243
8.3.1	Stretchable Nanofiber Mats	243
8.3.2	Stretchable Yarns and Fabrics	244
8.4	Application in Stretchable Electronics	247
8.4.1	Strain and Pressure Sensor	247
8.4.2	Organic Field-Effect Transistors	248
8.4.3	Optoelectronic Devices	252
8.5	Conclusions	254
	References	254
<b>9</b>	<b>Mechanics-Guided 3D Assembly of Flexible Electronics</b>	<b>265</b>
	<i>Guoquan Luo, Jianzhong Zhao, Xu Cheng, and Yihui Zhang</i>	
9.1	Introduction	265
9.2	Design Strategies of Mechanics-Guided Assembly	266
9.2.1	2D Precursor Designs	267
9.2.1.1	Origami/Kirigami Design Strategy	267
9.2.1.2	Multilayer and Multilevel Design Strategy	267
9.2.1.3	Design Strategy Based on Spatial Stiffness Control	269
9.2.2	Elastomer Substrate Designs	270
9.2.2.1	Engineered Planar Substrate Design Strategy	270
9.2.2.2	Curvilinear Substrate Design Strategy	272
9.2.3	Strategy of Loading Conditions	272
9.2.3.1	Mechanical Loading Strategy	272
9.2.3.2	Electric/Magnetic-Field-Assisted Loading Strategy	274
9.3	Mechanics Modeling and Analyses of the 3D Assembly	275
9.3.1	Buckling Analysis of 2D Precursors	275
9.3.1.1	Straight Ribbons	275
9.3.1.2	Helical Structures	277
9.3.1.3	Frame Structures	278
9.3.1.4	2D Curved Ribbons	278
9.3.2	Interfacial Adhesion in the Mechanics-Guided Assembly	279
9.3.2.1	Design Diagrams of Delamination States	279
9.3.2.2	Controlled Interface Delamination	281
9.3.3	Loading-Path Controlled Assembly	282
9.3.3.1	Reconfigurable Cross-Shaped Structures	282
9.3.3.2	Reconfigurable Structures Harnessing Interface Mechanics	282
9.4	Applications of 3D Flexible Electronics	284
9.4.1	Flexible Sensors	284

9.4.2	Tunable Electromagnetic Devices	284
9.4.3	Biomedical Devices	286
9.4.4	Flexible Robotics	286
9.5	Concluding Remarks	287
	References	288

## **10 Harnessing Wrinkling and Buckling Instabilities for Stretchable Devices and Healthcare** 293

*Yao Zhao, Fangjie Qi, Haoze Sun, Yanbin Li, Haitao Qing, and Jie Yin*

10.1	Introduction	293
10.2	Structural Designs and Mechanics	294
10.2.1	Structural Designs for Buckling-Enabled Stretchability	294
10.2.2	Mechanics of Wrinkling and Buckling	296
10.2.2.1	Compression-Induced Wrinkling	297
10.2.2.2	Compression-Induced Constrained Buckle-Delamination	298
10.2.2.3	Compression-Induced Spontaneous Buckle-Delamination	298
10.2.2.4	Tension-Induced Buckling in Serpentine Structures	299
10.2.2.5	Tension-Induced Buckling in Kirigami Structures	300
10.3	Applications in Stretchable Devices	300
10.3.1	Stretchable Sensors	300
10.3.2	Stretchable Batteries	302
10.3.3	Other Stretchable Electronics	304
10.4	Applications in Healthcare	306
10.4.1	Biosensors	306
10.4.2	Biological Interfaces	308
10.5	Conclusion and Outlook	311
	Acknowledgments	311
	References	311

## **Part III Applications** 319

### **11 Spherical Indentation Behavior of Soft Electronics** 321

*Changxian Wang, Zequn Cui, and Xiaodong Chen*

11.1	Spherical Indentation of the Semi-infinite Solid	321
11.1.1	General Solution for Elastic Solid with Displacement Function	321
11.1.2	Indentation Behavior of Revolution Indenter	325
11.1.3	Indentation Behavior of Spherical Indenter	327
11.2	Applications in a Force-Softness Bimodal Sensor Array for Human Body Feature Identification	328
11.2.1	Design of the Spherical Indenter-Based Force-Softness Sensor	329
11.2.1.1	The First Stage	331
11.2.1.2	The Second Stage	332
11.2.2	Integration of the Force-Softness Sensor Array: Tactile Glove	334
11.2.3	Applications in Body Feature Identification	336

11.3	Applications in a Self-Locked Young's Modulus Sensor for Quantifying the Softness of Swollen Tissues in the Clinic	336
11.3.1	Design of the Fingertip Modulus Sensor	337
11.3.2	Applications in Softness Measurement of Swollen Tissues in the Clinic	340
11.4	Conclusions	343
	References	343
<b>12</b>	<b>Mechanics of Wet Adhesion</b>	<b>345</b>
	<i>Jiawei Yang and Ruobing Bai</i>	
12.1	Introduction	345
12.2	Characterization of Adhesion	346
12.3	General Principles for Strong Wet Adhesion	347
12.3.1	Chemistry of Bonds	349
12.3.1.1	Static Covalent Bonds	349
12.3.1.2	Dynamic Covalent Bonds	349
12.3.1.3	Ionic Bonds	349
12.3.1.4	Hydrogen Bonds	350
12.3.1.5	Hydrophobic Interaction	350
12.3.1.6	$\pi$ - $\pi$ Stack	351
12.3.1.7	Dipole-Dipole Interaction	351
12.3.1.8	Host-Guest Interaction	351
12.3.1.9	Catechol Chemistry	351
12.3.2	Topology of Connection	351
12.3.3	Mechanics of Dissipation	352
12.4	Methods for Strong Wet Adhesion	354
12.5	Mechanics of Wet Interfaces	357
12.5.1	Adhesive Failure and Cohesive Failure	357
12.5.2	Fractocohesive Length- and Size-Dependency	358
12.5.3	Rate Dependency	359
12.5.4	Fatigue	360
12.5.5	Stretchable Adhesion	361
12.6	Summary and Outlook	362
	References	363
<b>13</b>	<b>Electromechanics of Soft Resistive and Capacitive Tactile Sensors</b>	<b>373</b>
	<i>Zhengjie Li, Sangjun Kim, Zheliang Wang, Zhengtao Zhu, and Nanshu Lu</i>	
13.1	Introduction	373
13.1.1	Overview of Tactile Sensors	373
13.1.2	Bottlenecks of Soft Resistive and Capacitive Tactile Sensors	376
13.2	Resistive Tactile Sensors	378
13.2.1	Introduction of Resistive Tactile Sensors	378
13.2.2	Resistive Tactile Sensors Based on Microstructured Contact	379

13.2.3	Resistive Tactile Sensors Based on Bulk Conductive Nanocomposites	385
13.2.4	Resistive Tactile Sensors Based on Porous Conductive Materials	392
13.2.5	Stretchable Resistive Tactile Sensors	397
13.3	Capacitive Tactile Sensors	399
13.3.1	Introduction of Capacitive Tactile Sensors	399
13.3.2	Capacitive Tactile Sensors with Engineered Dielectrics	401
13.3.3	Capacitive Tactile Sensors with Engineered Electrodes	408
13.3.4	Stretchable Capacitive Tactile Sensors	413
13.4	Resistive–Capacitive Hybrid Response Tactile Sensors	415
13.4.1	Flexible Hybrid Response Tactile Sensors	415
13.4.2	Stretchable Hybrid Response Tactile Sensors	417
13.5	Conclusion and Outlook	418
13.5.1	Summary of the Existing Achievements	418
13.5.2	Remaining Challenges and Future Prospects	419
	Acknowledgments	420
	References	420

## **14 Active Mechanical Haptics Constructed with Curved Origami** 431

*Zhuang Zhang and Hanqing Jiang*

14.1	Introduction	431
14.2	Stiffness Tuning via Curved Origami	432
14.3	Theoretical Modeling and Analysis of Curved Origami	434
14.3.1	Geometric Modeling	434
14.3.2	Mechanics Modeling	436
14.3.3	Active Tuning	437
14.4	Closed-Loop Design and System Integration of Origami	438
14.5	In-hand Haptic Device	440
14.6	Stiffness Perception via Active Pressing	443
14.7	Body-Centered Stepping Device	444
14.8	Whole-Body Stiffness Perceptions	447
14.9	Discussion	448
	References	450

## **15 Mechanics of Transient Electronics** 453

*Ankan Dutta and Huanyu Cheng*

15.1	Introduction	453
15.2	Hydrolysis of Semiconducting Materials	455
15.3	Model of Reactive Diffusion for Transient Materials	457
15.4	Dissolution of the Device with Bi-layered Structures	461
15.5	Conclusion	467
	Acknowledgments	468
	References	468

## **Index** 473

## Preface

Flexible and stretchable electronics represent an emerging technology with the potential to significantly impact a wide array of areas including healthcare, energy, robotics, manufacturing, and defense. Unlike rigid electronics, this technology enables novel applications ranging from wearable or implantable devices to soft robots. Although many interdisciplinary challenges exist in this field, a fundamental challenge is achieving mechanical flexibility, stretchability, or surface conformability while maintaining the functionalities and performance of the electronics.

The mechanics of materials, structures, and interfaces plays a crucial role in addressing this challenge. This book aims to showcase some successful and nascent approaches including soft functional materials (such as composites, nanomaterials, organic semiconductors, hydrogels, liquid metals, and so on), soft structures (like origami/kirigami, serpentines, wrinkles, buckles, architected materials, etc.), and advanced bio-electronics adhesives, among others. The focus throughout is on the mechanistic understandings and/or the mechanics-driven designs of such materials, structures, interfaces, and systems.

Recent books in the field of flexible and stretchable electronics largely focus on materials, manufacturing, electronics, and applications. However, the mechanics underlying these advancements have been instrumental in the rapid progress of this field. We believe that a book summarizing the recent developments in this crucial aspect is both timely and necessary.

Our primary audience includes senior undergraduate students, graduate students, and early-stage researchers who are interested about the mechanics of soft electronics or planning to take it on as their research directions. Additionally, instructors teaching undergraduate and graduate courses on the topic will find valuable resources within these chapters. Anticipated readers may come from a wide range of disciplines including, but not limited to, mechanics, physics, materials science, chemical engineering, electronics, and biomedicine, reflecting the multidisciplinary nature of flexible and stretchable electronics.

Authored by leading experts, this book is divided into three parts, comprising 15 chapters. Part I (Chapters 1–5) addresses the mechanics of a variety of materials commonly used in flexible and stretchable electronics such as hydrogels, 1-D and 2-D nanomaterials, liquid metals, and organic semiconductors. Part II (Chapters 6–10) explores the mechanics involved in the design and manufacturing

of these electronics, covering diverse structural designs like mechanics-guided 3D assembly and wrinkling/buckling instabilities, and manufacturing processes including laser-based methods and electrospinning. Part III (Chapters 11–15) delves into mechanics issues relevant to applications, such as the indentation behavior of soft electronics, wet adhesion, and the integration of mechanics in applications like tactile sensors, haptics with curved origami, and transient electronics. These 15 chapters provide a snapshot of the recent advancements in the mechanics of flexible and stretchable electronics.

We extend our sincere gratitude to all contributing authors, whose dedication and hard work made this book possible. We are also indebted to the editorial team at Wiley-VCH for their exceptional technical assistance.

June 2024

*Yong Zhu and Nanshu Lu  
Raleigh and Austin*



## **Part I**

### **Materials**



## 1

## Extreme Mechanics of Hydrogels Toward *In Situ* Hydrogel Bioelectronics

Tsz H. Wong<sup>1</sup>, Xuanhe Zhao<sup>2,3</sup>, and Shaoting Lin<sup>4</sup>

<sup>1</sup>Michigan State University, Department of Biomedical Engineering, 775 Woodlot Dr., East Lansing, MI 48824, USA

<sup>2</sup>Massachusetts Institute of Technology, Department of Mechanical Engineering, 77 Massachusetts Avenue, Cambridge, MA 02139, USA

<sup>3</sup>Massachusetts Institute of Technology, Department of Civil and Environmental Engineering, 77 Massachusetts Avenue, Cambridge, MA 02139, USA

<sup>4</sup>Michigan State University, Department of Mechanical Engineering, 474 S Shaw Ln, East Lansing, MI 48824, USA

### 1.1 Introduction

*In-situ* bioelectronics, a rapidly evolving field focusing on the development of electronic devices that can operate within the body for on-site sensing, stimulation, and powering, holds great promise for revolutionizing the field of medicine in a variety of ways (Figure 1.1a) [1, 2]. For example, the development of biosensors that can achieve on-site quantification of biomarkers closely related to the development and progression of colorectal cancer (CRC) would enable early CRC detection preventing CRC from progressing, thereby increasing the five-year relative survival rate up to 90% [3]. The development of neural probes that can form intimate interfaces with neurons without provoking a severe foreign body response would enable chronic neuron stimulation and recording, facilitating fundamental understanding of neural activities and offering long-term treatment for neuropsychiatric disorders, traumatic injuries, and inflammatory conditions [4–6]. The advancement of energy harvesting devices that can provide sustainable power supply to cardiac pacemakers could prolong their lifespan and help maintain or restore a normal heart rhythm with electrical impulses [7–9]. However, the key challenge faced by *in-situ* bioelectronics stems from the fundamentally contradictory properties between electronic components and biological systems, which induce foreign body responses due to mechanical, chemical, and biological mismatches. Specifically, electronic components are typically made of metals, silicon, glass, ceramics, and plastics that are hard, dry, and abiotic; in contrast, biological systems are composed of living tissues that are soft, wet, and dynamic.

Hydrogels, as polymer networks infiltrated with water, exhibit intriguing multiphysics phenomena associated with mechanical, electrical, chemical, and thermal

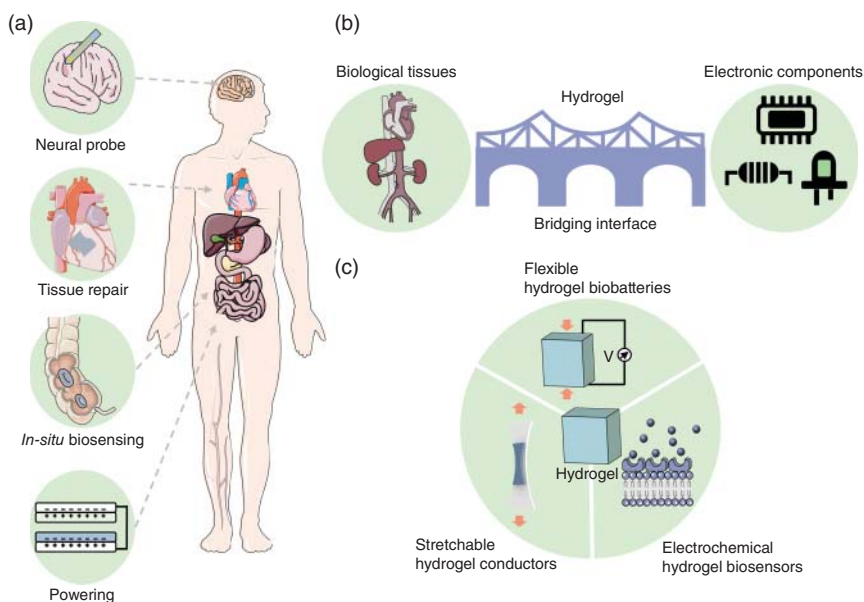


**Figure 1.1** Overview of the *in-situ* hydrogel electronics. (a) *In-situ* bioelectronics revolutionized the field of medicine in a variety of ways. (b) Hydrogels form long-term, high-efficacy, multi-modal bridging interfaces between electronic components and biological systems. (c) Three key components of *in-situ* hydrogel bioelectronics include stretchable hydrogel conductors, electrochemical hydrogel biosensors, and flexible hydrogel biobatteries.

couplings [10, 11]. Hydrogels are typically constituted of two phases: one phase of interconnected polymer networks giving the solid-like network elasticity, and the other phase of infiltrated water molecules endowing the fluid-like transport property [12–15]. Due to the unique combination of polymer networks and water molecules, hydrogels show their superior softness, wetness, responsiveness, biocompatibility, and bioactivity, therefore having been regarded as an ideal material candidate to form long-term, high-efficacy, multi-modal bridging interfaces between electronic components and biological systems (Figure 1.1b) [16, 17].

Recently, a nascent field named hydrogel bioelectronics has rapidly evolved, exploiting hydrogels as key components for electronic devices that seamlessly interact with biological systems. The generic idea for the design of hydrogel bioelectronic device is to embed functional electronic components such as conductors, microchips, transducers, resistors, and capacitors inside or attached to the surface of a highly stretchable and tough hydrogel matrix, providing a soft, wet, and biocompatible environment interfacing with biological tissues [18]. As the hydrogel bioelectronic device is stretched, flexible electronic components can deform together with the device while rigid electronic components maintain their undeformed shapes, which involves large deformation of hydrogels around rigid electronic components [19, 20]. Therefore, to maintain reliability and functionality of the device, the hydrogel matrix and the interface between hydrogel and

functional components need to be tough and robust. Pioneered by Gong et al., hydrogels with fracture toughness higher than  $10^4 \text{ J/m}^2$  have been widely available [21–23]; additionally, initiated in the past 10 years, hydrogel adhesions to diverse substrates can successfully achieve interfacial fracture toughness above  $10^3 \text{ J/m}^2$ , on the same order as their biological counterparts [24–29]. The recent development of tough hydrogels and tough hydrogel adhesions as well as their synthesis and fabrication techniques have enabled various soft material technologies in the form of diverse hydrogel bioelectronics [18, 30, 31].

More recently, an emerging class of *in-situ* bioelectronics that combines hydrogel technologies with electronic components to create devices that can interact with harsh environments within the body, which we define as *in-situ hydrogel bioelectronics*, have been recently proposed with great promise in potentially addressing the limitations faced by existing *in-situ* bioelectronics [16, 31, 32]. Despite the promise, the complicated chemical, biological, and mechanical factors in the physiological environment pose significant challenges to the reliability and functionality of hydrogel electronic devices when operating within the body. What are the key properties of hydrogels and how to rationally design these properties for developing electronic devices that can operate in the physiological environment for reliable on-site sensing, stimulation, and powering? These are unanswered questions, even considering a growing number of reviews on hydrogel bioelectronics [16, 33–37].

This chapter aims to provide an overview of the design principles, implementation mechanisms, and manufacturing/fabrication techniques, particularly centering on extreme mechanics of hydrogels, for developing three key components of *in-situ* hydrogel bioelectronics (Figure 1.1c): (i) stretchable hydrogel conductors, (ii) electrochemical hydrogel biosensors, and (iii) flexible hydrogel biobatteries. The chapter is organized as follows. Section 1.2 will discuss polymer mechanics for rationally designing extreme mechanical and physical properties of hydrogels crucial for the development of *in-situ* hydrogel bioelectronics. Section 1.3 will discuss the multiscale orthogonal design of stretchable hydrogel conductors and strategies for implementing the orthogonal design. Section 1.4 will discuss the principles for achieving high-specificity and high-sensitivity of electrochemical hydrogel biosensors, specifically focusing on selective transport design in hydrogels and electrochemical sensing performance at hydrogel–electrode interfaces. Section 1.5 will briefly review the recent efforts in developing flexible hydrogel biobatteries by harvesting mechanical energy, chemical energy, and thermal energy. Section 1.6 will conclude the chapter with a set of future opportunities by integrating interdisciplinary efforts in ingestible sensors, neural interfaces, miniature robots, and data analytics.

## 1.2 Extreme Properties of Hydrogels by Polymer Network Design

Due to the unique combination of solid-like polymer networks and fluid-like water molecules, hydrogels exhibit superior softness, wetness, responsiveness,

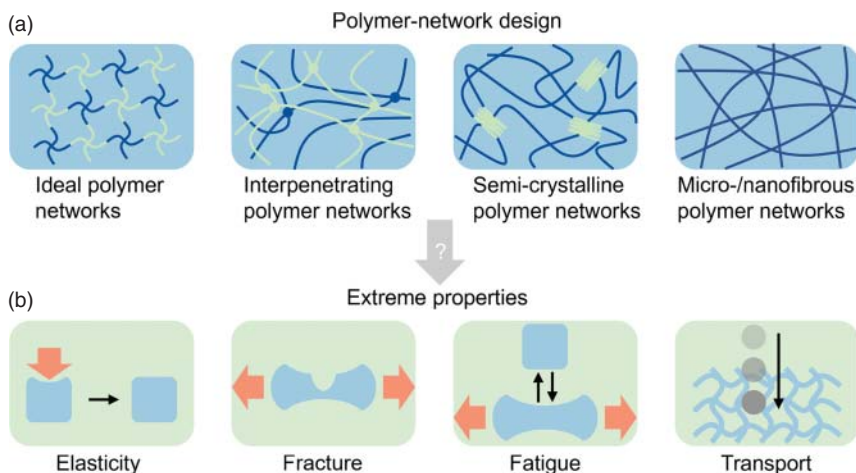


**Figure 1.2** Extreme properties of hydrogels by polymer network design. (a) Schematics of unconventional polymer networks such as ideal polymer networks, interpenetrating polymer networks, semi-crystalline polymer networks, micro-/nanofibrous polymer networks. (b) Schematics of mechanical and physical properties critical for the development of *in-situ* hydrogel bioelectronics, including elasticity, fracture, fatigue, and mass transport.

biocompatibility, and bioactivity, therefore being exploited as key material candidates for developing *in-situ* hydrogel bioelectronics. These properties have been intensively studied by understanding the nonlinear elasticity [38], swelling [39–43], poroelasticity [44, 45], viscoelasticity [46–50], fracture [51–53], and fatigue [54–57] of hydrogels, following the pioneering work in the field of polymers and soft materials [58–69]. Despite these unique mechanical and physical properties of common hydrogels, the development of *in-situ* hydrogel bioelectronics also requires hydrogels to possess extreme mechanical and physical properties, such as tunable elastic modulus, extremely high values of fracture toughness and fatigue threshold, and tunable molecular transport. In this section, we will discuss the polymer mechanics to rationally push the limits of mechanical and physical properties of hydrogels including elastic modulus, fracture toughness, fatigue threshold, and mass transport that are crucial for the development of *in-situ* hydrogel bioelectronics (Figure 1.2).

### 1.2.1 Elastic Modulus

Elastic modulus is one of the most important properties of hydrogels used in biomedical applications, as it governs their ability to withstand deformations while maintaining compliance without damaging the surrounding soft tissues or causing adverse foreign body responses. There are several methods available to measure the elastic modulus of hydrogels, including tensile/compression, rheology, and indentation tests, as illustrated in Figure 1.3a. The shear elastic modulus of a hydrogel  $G$  can be measured by identifying the initial slope of the stress–strain curve in tensile or compression tests  $E$ , namely  $G = \alpha E$ , where  $\alpha$  is a dimensionless perfector

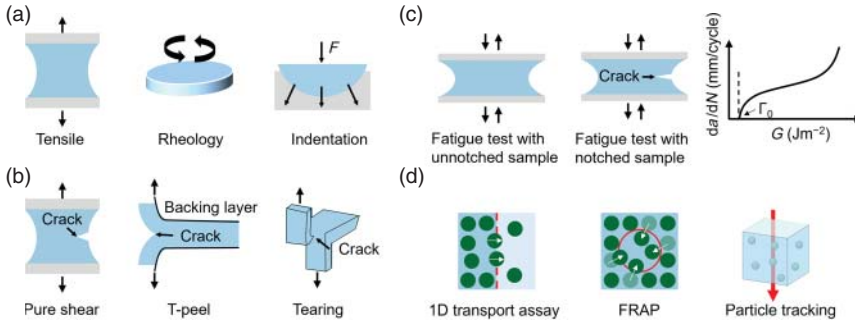


**Figure 1.3** Common experimental methods to characterize mechanical and physical properties of hydrogels. (a) Tensile, rheology, and indentation tests to measure the elastic modulus of hydrogels. (b) Pure shear, T-peel, and tearing tests to measure the fracture toughness of hydrogels. (c) Pure shear fatigue tests to measure the fatigue threshold of hydrogels  $\Gamma_0$  by plotting the crack extension  $da/dN$  versus the applied energy release rate  $G$ . (d) 1D transport assay, fluorescence recovery after photobleaching (FRAP), and particle tracking methods to measure the diffusivity of particles (e.g. ions, monomers, proteins, viruses) in hydrogels.

depending on samples' dimensions and material incompressibility [70]. Rheology test is the other method to measure the shear elastic modulus of a hydrogel, which is often preferred for soft hydrogels. Rheology tests can provide information on both storage and loss modulus across a range of frequencies, allowing for a quantitative decomposition of elastic and viscous contributions during deformation [71]. Indentation tests can also be used to characterize the shear elastic modulus, but the results may be affected by water migration and stress state. Therefore, a theoretical analysis is necessary to accurately interpret the indentation results and decouple nonlinear elasticity, viscoelasticity, and poroelasticity in hydrogels [72].

Assuming the polymer network of a hydrogel is fully amorphous with negligible molecular entanglements and crystalline domains, the shear elastic modulus of a hydrogel  $G$  can be theoretically predicted following the classical affine and phantom network theories of elasticity [12, 66],

$$\frac{G}{kT} = C\phi^{1/3}n \quad (1.1)$$

where  $\phi$  is the volume fraction of dry polymers,  $n$  is the number of elastically active polymer chains per unit volume of dry polymers,  $k$  is the Boltzmann constant,  $T$  is the absolute temperature, and  $C$  is a constant that has a value of 1 when the polymer network of the hydrogel follows affine deformation and  $1 - \frac{2}{f}$  when the polymer network of the hydrogel follows phantom deformation with  $f$  being the functionality of the polymer network (i.e. the number of chains connected to a junction point). By substituting the typical values of  $C = 1$ ,  $\phi = 0.1$ ,  $n = 10^{24} - 10^{26} \text{ m}^{-3}$ , and  $kT = 4.11 \times 10^{-21} \text{ J}$ , the shear elastic modulus of a hydrogel is estimated on the order of 1–100 kPa.

Recent experiments have shown that the measured shear modulus of a hydrogel is consistently below the theoretical predictions by Eq. (1.1) due to the presence of molecular defects in a real hydrogel. Given the capability of counting the numbers

of various orders of molecular defects in hydrogels, Olsen and Johnson and coworkers [73] developed a real elastic network theory to quantify the impact of molecular defects on shear elastic modulus,

$$\frac{G}{kT} = \frac{f-2}{f} \sum_i \varepsilon_i n_i \quad (1.2)$$

where  $n_i$  is the number of the type  $i$  polymer chains per unit volume of the hydrogel associated with a specific type of molecular defects,  $\varepsilon_i$  is the elastic effectiveness of the type  $i$  polymer chains.  $\varepsilon_i$  accounts for the elastic contribution of each polymer chain, having a value of 1 if the polymer chain is an ideal chain with no impact from defects and a value smaller than 1 if the polymer chain is a defective chain affected by surrounding molecular defects. The real elastic network theory suggests the critical role of polymer network architecture on hydrogel's elastic modulus. The design principle for achieving tunable elastic modulus of hydrogels is to engineer the type and density of molecular defects, ubiquitous in synthetic hydrogels and biological tissues [74] (Figure 1.4a).

### 1.2.2 Fracture Toughness

Fracture toughness, the energy required to propagate a unit area of crack surface under monotonic load, defines the ability of a material to resist crack extension under stress. Fracture toughness of a hydrogel is crucial for maintaining reliability of *in-situ* hydrogel bioelectronics [10, 11]. As illustrated in Figure 1.3b, the fracture toughness of a hydrogel can be measured through pure shear, T-peel, and tearing tests, originally proposed by Rivlin and Thomas for measuring the fracture toughness of rubbers [75]. In a pure shear test, the fracture toughness of a hydrogel  $\Gamma$  is determined by the critical energy release rate applied on a notched sample  $G_c$ ,  $\Gamma = G_c = W(\lambda_c)H$ , where  $W$  is the strain energy density stored in the unnotched sample with  $\lambda_c$  being the critical stretch for crack extension in the notched sample, and  $H$  is the sample height [53]. T-peel tests can also be used to measure the fracture toughness of hydrogels [76], where a hydrogel layer with a precut is sandwiched between two inextensible backing layers. The fracture toughness of the hydrogel is then calculated via  $\Gamma = 2F_{SS}/b$ , where  $F_{SS}$  is the steady-state plateau force, and  $b$  is the specimen's thickness. Tearing tests, also known as trouser tests, are another commonly adopted method for measuring hydrogel toughness [77]. Unlike pure shear and T-peel tests with the crack deformed in Mode I, the crack in a tearing test is deformed in Mode III (out-of-plane shear loading). The fracture toughness of a hydrogel in a tearing test is determined by  $\Gamma = 2F_{SS}/b$ , where  $F_{SS}$  is the steady-state plateau force, and  $b$  is the specimen's thickness.

Common hydrogels are intrinsically brittle [78]. The intrinsic fracture energy of a hydrogel  $\Gamma_0$  can be calculated following the classical Lake-Thomas theory [12, 61, 79],

$$\Gamma_0 = \phi^{2/3} \cdot n\sqrt{Nb} \cdot NU = \phi^{2/3} nbN^{3/2}U \quad (1.3)$$

where  $\phi$  is the volume fraction of dry polymers,  $n\sqrt{Nb}$  is the number of elastically active polymer chains per unit area of crack surface, with  $n$  being the number of



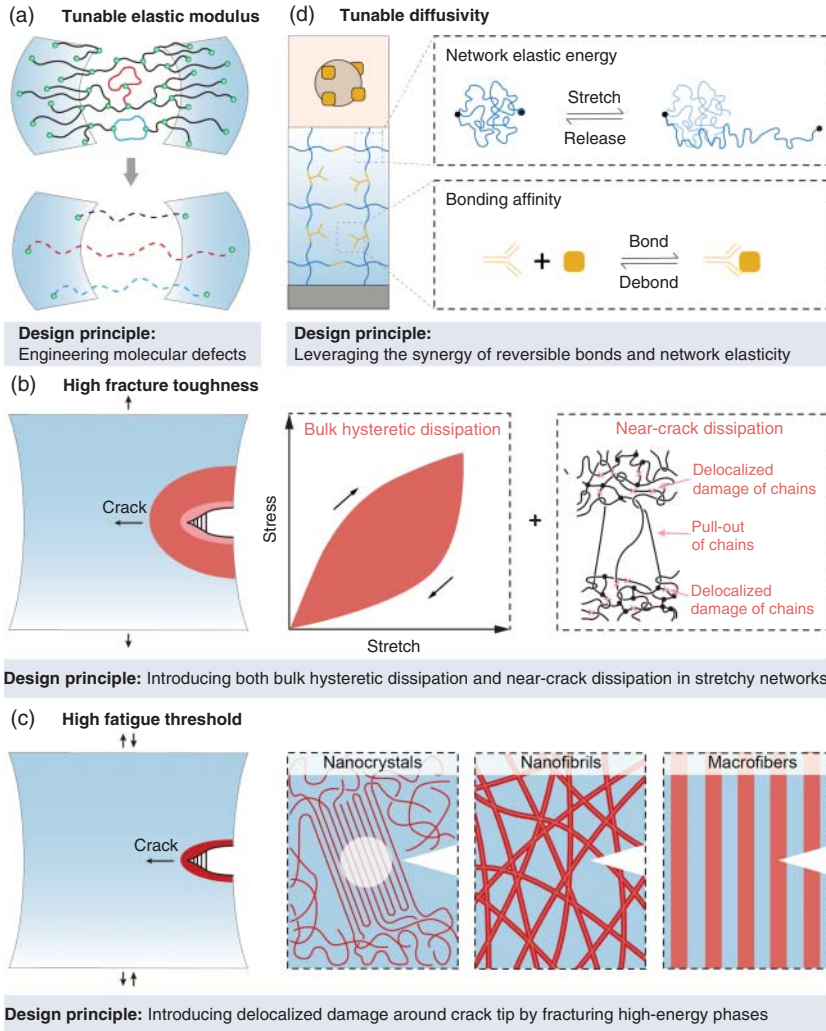


**Figure 1.4** Design principles for extreme properties of hydrogels. (a) Achieving tunable elastic modulus by engineering type and density of molecular defects in hydrogels. (b) Achieving high fracture toughness of hydrogels by introducing both bulk hysteretic dissipation and near-crack dissipation in stretchy polymer networks. (c) Achieving high fatigue threshold of hydrogels by introducing high-energy phases to impinge fatigue crack extension. (d) Achieving tunable diffusivity in hydrogels by leveraging the synergy of reversible bonds and network elasticity.

elastically active polymer chains per unit volume of dry polymers,  $N$  being the number of Kuhn monomers in each polymer chain,  $b$  being the length of each Kuhn monomer,  $Nb^3 = 1$  with  $b^3$  being the volume of a Kuhn monomer. It is commonly assumed that the dry polymers of a hydrogel satisfy the volume conservation following  $Nnb^3 = 1$  with  $b^3$  being the volume of a Kuhn monomer. By imposing the volume conservation, the

intrinsic fracture energy of a hydrogel can be calculated via,

$$\Gamma_0 = \phi^{2/3} b^{-2} N^{1/2} U \quad (1.4)$$

By substituting the typical values of  $\phi = 0.1$ ,  $b = 10^{-9}$  m,  $N = 100 - 10,000$ , and  $U = 100kT = 4.11 \times 10^{-19}$  J, the intrinsic fracture energy of a hydrogel  $\Gamma_0$  is estimated as low as 1–10 J/m<sup>2</sup>, orders of magnitude lower than biological tissues around 1000 J/m<sup>2</sup>.

Lin and Zhao recently developed a defect-network fracture model to predict the intrinsic fracture energy of polymer networks containing various types of topological defects including cyclic loops and dangling chains [80]. The defect-network fracture model is inspired by the real elastic network model [73] or, more generally, the phantom network model [66, 81] discussed in Section 1.2.1. Analogous to the previous elastic models, the key idea of this fracture model is to introduce effectively longer fractured chains to account for the energy of the fractured chains on the crack path. However, physically different from the previous elastic models, the effectively longer chains in the fracture model do not change the density of the layer of fractured chains. The intrinsic fracture energy of the polymer network with defects normalized by that of the corresponding defect-free ideal network can be expressed as:

$$\bar{\Gamma} = \sum_X (\gamma_X - 1) n_X^{\text{affected}} - \sum_X n_X^{\text{inactive}} + 1 \quad (1.5)$$

where  $\gamma_X \geq 1$  is the fracture effectiveness to account for the contribution to intrinsic fracture toughness by a single polymer chain affected by defect  $X$ ,  $n_X^{\text{affected}}$  is the number density of affected chains due to the presence of defect  $X$ ,  $n_X^{\text{inactive}}$  is the number density of inactive chains due to the presence of defect  $X$ . The defect-network fracture model indicates a competing effect due to the presence of topological defects: toughening by increasing effective chain length and weakening by introducing inactive chains. While the defect-network fracture model predicts that the presence of defects can potentially enhance intrinsic fracture energy of hydrogels by a few times, such enhancement is not sufficient to ensure the reliable use of hydrogels in engineering applications.

In the past 20 years, the fracture toughness of hydrogels has been significantly enhanced above 1000 J/m<sup>2</sup>, making tough hydrogels key load-bearing components for devices and machines [82, 83]. The generic toughening mechanism of hydrogels is to incorporate two physical processes: one is the scission of a layer of polymer chains on the crack tip, and the other is the bulk hysteretic dissipation around the crack tip such as Mullins effect and viscoelasticity [22, 23, 51, 78, 84–91]. The first process defines the intrinsic fracture energy  $\Gamma_0$  as discussed in Eqs. (1.3)–(1.5), and the second process defines the bulk hysteretic dissipation's contribution  $\Gamma_D^{\text{bulk}}$ . Conceptually, the total fracture toughness of a tough hydrogel can be expressed as:

$$\Gamma = \Gamma_0 + \Gamma_D^{\text{bulk}} \quad (1.6)$$

which is often named the bulk dissipation model. The value of  $\Gamma_D^{\text{bulk}}$  can be estimated by  $\Gamma_D^{\text{bulk}} = U_D L_D$  with  $U_D$  being the energy for breaking sacrificial bonds per unit volume of the material and  $L_D$  being the length of the process zone around crack tip where breaking sacrificial bonds occurs.  $U_D$  can be estimated by the bond

energy of one sacrificial bond times the number of sacrificial bonds per unit volume of the material, on the order of  $10^6 \text{ J/m}^3$ . Since the value of  $L_D$  can reach 1 mm [92], the value of  $\Gamma_D^{\text{bulk}}$  can reach  $1000 \text{ J/m}^2$ , with the orders of magnitude larger than  $\Gamma_0$ .

The bulk dissipation model has been widely used to qualitatively explain the toughening mechanisms in diverse soft tough materials [21, 23, 93–95], but recent study shows that the bulk dissipation model significantly underestimates the toughness enhancement of tough hydrogels [93]. The missing term is attributed to a near-crack dissipation that does not rely on bulk hysteresis [96–98]. To account for both bulk hysteretic dissipation and near-crack dissipation in soft tough materials, an extreme toughening model was recently proposed, indicating that the total fracture toughness of a tough hydrogel exhibiting both bulk hysteretic dissipation and near-crack dissipation can be expressed as:

$$\Gamma = \Gamma_0 + \Gamma_D^{\text{bulk}} + \Gamma_D^{\text{tip}} \quad (1.7)$$

where  $\Gamma_0$  is the intrinsic fracture energy,  $\Gamma_D^{\text{bulk}}$  is the bulk hysteretic dissipation's contribution to fracture toughness, and  $\Gamma_D^{\text{tip}}$  is the near-crack dissipation's contribution to fracture toughness. A governing equation for the extreme toughening model can be further derived as:

$$\frac{\Gamma}{\Gamma_0} = \frac{\beta}{1 - \alpha h_m} \quad (1.8)$$

where  $\beta = (\Gamma_0 + \Gamma_D^{\text{tip}})/\Gamma_0 \geq 1$  is a dimensionless number to account for the near-crack dissipation due to molecular entanglements,  $0 \leq \alpha \leq 1$  is a dimensionless number depending on the stretch-dependent hysteresis of the bulk materials ( $\alpha = 1$  for highly stretchable materials), and  $0 \leq h_m < 1$  is the maximum stress-stretch hysteresis of the bulk material. While the cause of the near-crack dissipation is not fully understood, the reported experiments have shown the potential for achieving high values of  $\beta$  up to 10, suggesting the crucial toughening role by the near-crack dissipation. To summarize, the design principle for achieving high fracture toughness in hydrogels is to introduce both bulk hysteretic dissipation (e.g. Mullins effect and viscoelasticity) and near-crack dissipation (e.g. molecular entanglements) in stretchy polymer networks, as depicted in Figure 1.4b.

### 1.2.3 Fatigue Threshold

Fatigue threshold, the energy required to propagate a unit area of crack surface under cyclic load, defines the ability of a material to resist fatigue crack extension under stress [55, 99, 100]. Fatigue threshold of hydrogels is critical for achieving longevity of *in-situ* hydrogel bioelectronics. As illustrated in Figure 1.3c, the measurement of fatigue threshold of hydrogels requires cyclic loading of unnotched and notched hydrogel specimens. The fatigue tests for hydrogels are typically performed in a chamber with controlled humidity or water bath to ensure the sample reaches an equilibrium state [54, 56]. By monitoring the crack extension  $\Delta a$  at a controlled

energy release rate  $G$ , one can identify a critical energy release rate at the intersection of abscissa axis as the measured fatigue threshold  $\Gamma_0$ .

While hydrogels have been made tough with high toughness above  $1000 \text{ J/m}^2$ , as discussed in Section 1.2.2, these tough hydrogels still suffer from fatigue fracture when subjected to prolonged cyclic loading [54, 79, 97, 101]. The experimental findings conclude that the resistance to fatigue crack propagation after prolonged cycles of loads is the energy required to fracture a single layer of polymer chains (i.e. the intrinsic fracture energy of the hydrogel), which is unaffected by the additional dissipation mechanisms introduced in tough hydrogels [56]. To address the challenge of fatigue failures in conventional tough hydrogels, we and others have proposed a general design principle for fatigue-resistant hydrogels (Figure 1.4c) – inducing delocalized damage around the crack tip by fracturing high-energy phases, such as nanocrystals [28, 56, 100, 102–104], micro-/nanofibers [105], and macro-fibers [92, 106] in hydrogels. Additionally, hierarchical molecular structure design such as introducing bi-continuous phase networks can suppress fatigue-induced crack advance [57, 107].

The fatigue threshold of fatigue-resistant hydrogels containing high-energy phases can be qualitatively calculated by modifying the Lake–Thomas theory:

$$\Gamma_0 = \phi^{2/3} n l_d N U \quad (1.9)$$

where  $\phi$  is the volume fraction of dry polymers,  $n$  is the number of elastically active polymer chains per unit volume of dry polymers,  $NU$  is the energy required to fracture a polymer chain with  $N$  being the number of Kuhn monomers in each polymer,  $U$  being the energy required to fracture a single Kuhn monomer, and  $l_d$  is the length scale of the delocalized damage and understood as the crack processing zone length at the threshold. In conventional hydrogels,  $l_d$  is equal to the length of a single layer of polymer chains, i.e.  $l_d = \sqrt{Nb}$ ; in fatigue-resistant hydrogels,  $l_d$  is larger than the length of a single layer of polymer chains, i.e.  $l_d > \sqrt{Nb}$ . Since the parameters  $\phi$ ,  $N$ , and  $U$  are intrinsic properties of hydrogels with little room to engineer, the strategies to enhance fatigue threshold of hydrogels mainly rely on the mechanisms that can significantly enlarge the value of  $l_d$ , which can be achieved by introducing intrinsically high-energy phases above mentioned.

#### 1.2.4 Mass Transport

Diffusion in a hydrogel, movement of particles (e.g. ions, monomers, proteins, and viruses) through the hydrogel, is a ubiquitous phenomenon in nature and a fundamental process that governs the working principles in diverse applications. For example, the distinct diffusion of different biomarkers in hydrogels determines the sensing sensitivity and sensing specificity in electrochemical hydrogel biosensors discussed in Section 1.4; the stress-induced diffusion of ions in nano channels of hydrogels governs the stress-voltage coupling in flexible hydrogel batteries discussed in Section 1.5. The diffusivity of particles in hydrogels can be commonly characterized by 1D transport assay, fluorescence recovery after bleaching (FRAP), and particle tracking methods (Figure 1.3d).

The mode of diffusion in a hydrogel is determined by the mesh size of the hydrogel. When the hydrogel's mesh size is much larger than the size of the substance, the substance moves as Brownian diffusion, the diffusivity of which is governed by the viscosity of solvent (i.e. water) in the hydrogel [108]:

$$D = \frac{kT}{3\pi\eta d} \quad (1.10)$$

where  $k$  is the Boltzmann constant,  $T$  is the absolute temperature,  $\eta$  is the dynamic viscosity of water, and  $d$  is the diameter of the substance. By substituting the typical values of  $kT = 4.21 \times 10^{-21}$  J,  $\eta = 8.9 \times 10^{-4}$  Pa · s, and  $d = 1$  nm, the diffusivity of the substance in a hydrogel with large mesh size is estimated as  $10^{-10}$  m/s<sup>2</sup>. When the hydrogel's mesh size is on the same order as the size of the substance, the diffusivity of the substance in a hydrogel is governed by the hydrogel's mesh size  $\xi$  [109]:

$$\frac{D}{D_0} \sim \exp\left(-\frac{d}{\xi}\right) \quad (1.11)$$

where  $D_0$  is the diffusivity of the substance in water. For a hydrogel with its mesh size two times the substance diameter (i.e.  $d/\xi = 2$ ), the diffusivity of the substance reduces by 10 times on the order of  $10^{-11}$  m/s<sup>2</sup>.

Existing efforts have been mostly focused on Brownian diffusion of particles in a fluid, the diffusivity of which is governed by the viscosity of fluids. In contrast, when particles diffuse in the polymer networks of a hydrogel, the transport of particles is a discrete process of particles making stochastic hops between neighboring sites, namely hopping diffusion, the diffusivity of which is governed by the energy required to overcome the elasticity of polymer networks [110]. Such network elasticity can be readily tuned by mechanical deformation applied on the hydrogel. This implies the potential of harnessing mechanical deformation as a new design space to program particle transport in hydrogels. Specifically, for a particle with size  $d$  confined in a cage formed by polymer chains with mesh size  $\xi$  slightly smaller than particle size (i.e.  $\xi < d$ ), the particle can still escape from one cage to the other neighboring cage by overcoming the energy barrier due to network elasticity. The probability for such escape  $P$  is determined by the energy barrier  $E_c$  via  $P = \int_d^\infty \frac{e^{-E_c/kT}}{\xi} dx$  where  $k$  is the Boltzmann constant and  $T$  is the absolute temperature, resulting in a reduced hopping diffusivity [110],

$$D_{\text{network}} = D_0 P \quad (1.12)$$

where  $D_0$  is the particle diffusivity in a hydrogel free of network elasticity. The fundamental understanding of how mechanical deformation modulates particle transport in soft materials remains an unexplored research topic but will potentially lead to multiple previously inaccessible technologies that rely on mechano-transport design in hydrogels, including but not limited to force-sensitive cargo for on-demand drug delivery, and strain-programmable tissue adhesive for prolonged tissue repair.

In addition to network elasticity, hopping diffusion in hydrogels can also be induced by reversible interactions between particles and functional groups in hydrogels [111]. During a hopping event, multipoint particle attachment results in caging. As one or more of the attached points can be released, the particle can escape from one cage to the other neighboring cage, resulting in hopping

diffusivity,

$$D_{\text{reversible}} = \sum_{j=2}^N k_{\text{off}} P_j D_0. \quad (1.13)$$

where  $P_j$  is the probability of a particle maintaining  $j$  number of bonding sites,  $N$  is the number of bonding sites on the particle,  $D_0$  is the particle diffusivity with one bonding site ( $N = 1$ ), and  $k_{\text{off}}$  is the dissociate rate of the reversible interaction. Harnessing hopping diffusion by reversible interactions enables selective transport of chemical and biological cargoes based on reversible cargo-barrier interactions [112, 113]. Overall, the principle to tune particle diffusivity in hydrogels is to leverage the synergy of network elasticity and reversible bonds (Figure 1.4d).

### 1.3 Stretchable Hydrogel Conductors

Hydrogel-based electronic materials that can conduct electricity while being able to stretch and deform without fracture, known as stretchable hydrogel conductors, hold great potential as an alternative to traditional metallic conductors in the development of *in-situ* hydrogel bioelectronics due to their unique combination of tissue-like properties and electrical conductivity [18, 114]. Despite the promising potential, existing stretchable hydrogel conductors face a technical challenge in reconciling superior mechanical toughness and high electrical conductivity, limiting their use in *in-situ* hydrogel bioelectronics that require both mechanical and electrical properties [115–117]. Currently, most stretchable hydrogel conductors consist of a mixture of electrically conductive fillers in stretchable hydrogel matrices, resulting in low electrical conductivity due to low connectivity between electrical phases in the hydrogel matrices. Although increasing the amount of conductive filler can improve the electrical conductivity by forming a percolation network, this approach significantly compromises the hydrogel's mechanical properties by reducing stretchability and fracture toughness.

#### 1.3.1 Multiscale Orthogonal Design

The design principle of stretchable hydrogel conductors is depicted in Figure 1.5, where the integration of electrical and mechanical phases is accomplished by a bi-continuous structure with an orthogonal design of each phase. To achieve high electrical conductivity, various electrical fillers such as ions [118, 119], conductive monomers [120, 121], conductive polymers [122–124], conductive nanoparticles [125, 126], and conductive macro fillers [127, 128] have been used. On the other hand, to achieve superior mechanical elasticity, stretchable hydrogels with interpenetrating polymer networks [21, 23, 129], hybrid crosslinkers [130–132], high-functionality crosslinkers [133–135], monodispersed polymer chains [136, 137], and meso-/macro composites [138–140] have been designed. While high electrical conductivity and superior mechanical elasticity have been